

# Identification by time-resolved EPR of the peridinin directly involved in chlorophyll triplet quenching in the peridinin–chlorophyll *a*–protein from *Amphidinium carterae*

Marilena Di Valentin <sup>a</sup>, Stefano Ceola <sup>a</sup>, Enrico Salvadori <sup>a</sup>,  
Giancarlo Agostini <sup>b</sup>, Donatella Carbonera <sup>a,\*</sup>

<sup>a</sup> Dipartimento di Scienze Chimiche, Università di Padova, via Marzolo 1, 35131 Padova, Italy

<sup>b</sup> CNR, Istituto di Chimica Biomolecolare, Sezione di Padova, via Marzolo 1, 35131 Padova, Italy

Received 31 July 2007; received in revised form 6 September 2007; accepted 7 September 2007

Available online 26 September 2007

## Abstract

The mechanism of triplet–triplet energy transfer in the peridinin–chlorophyll–protein (PCP) from *Amphidinium carterae* was investigated by time-resolved EPR (TR-EPR). The approach exploits the concept of spin conservation during triplet–triplet energy transfer, which leads to spin polarization conservation in the observed TR-EPR spectra. The acceptor (peridinin) inherits the polarization of the donor (chlorophyll) in a way which depends on the relative geometrical arrangement of the donor–acceptor couple. Starting from the initially populated chlorophyll triplet state and taking the relative positions among Chls and peridinin from the X-ray structure of PCP, we calculated the expected triplet state polarization of any peridinin in the complex. Comparison with the experimental data allowed us to propose a path for triplet quenching in the protein. The peridinin–chlorophyll pair directly involved in the triplet–triplet energy transfer coincides with the one having the shortest center to center distance. A water molecule, which is coordinated to the central Mg atom of the Chl, is also placed in close contact with the peridinin. The results support the concept of localization of the triplet state mainly in one specific peridinin in each of the two pigment subclusters related by a pseudo  $C_2$  symmetry.

© 2007 Elsevier B.V. All rights reserved.

**Keywords:** PCP; Carotenoid; Triplet; TR-EPR

## 1. Introduction

Photosynthesis is an important process which converts solar radiation into other types of energy directly exploitable by organisms. Light harvesting is the first step in photosynthesis and occurs in the protein–pigments complexes called antenna proteins, while the energy conversion step occurs in the reaction centers where the excitation energy is used to drive electrons across the photosynthetic membrane, creating an electrical po-

tential. Antenna complexes, which contains pigments such as (bacterio)chlorophylls, (B)Chls, and carotenoids, exhibit large structural and spectral variability, depending on the organisms. Marine algae contribute to photosynthetic CO<sub>2</sub> fixation. They possess an efficient light-harvesting system optimized for light-harvesting capacity especially in the blue-green spectral region because water functions as a filter of light in the red. The peridinin–chlorophyll *a*–protein (PCP) of the dinoflagellate *Amphidinium carterae*, belongs to the group of marine eukaryotic algae which employ carotenoids, such as peridinin, fucoxanthin, siphonaxanthin, characterized by the presence of a carbonyl group in their molecular structure, to fulfil their light-harvesting function. For these algae carotenoids play the major light-harvesting function. PCP is a water-soluble protein. The structure of PCP from the dinoflagellate *A. carterae* has been resolved to 2.0 Å [1]. It contains only peridinin and Chl *a* in a

**Abbreviations:** Per, peridinin; Chl, chlorophyll; PCP, peridinin–chlorophyll protein; ODMR, optically detected magnetic resonance; ZFS, zero field splitting; ISC, intersystem crossing; TR-EPR, Time-resolved Electron Paramagnetic Resonance; *A. carterae*, *Amphidinium cartarae*; MFPCP, main form PCP; HSPCP, high salt PCP

\* Corresponding author. Tel.: +39 049 827 5144; fax: +39 049 827 5161.

E-mail address: [donatella.carbonera@unipd.it](mailto:donatella.carbonera@unipd.it) (D. Carbonera).

stoichiometric ratio of 4:1. The basic structure is a trimer. In each subunit of the trimer the pigments are arranged as two pseudo-identical domains of four peridinin and one Chl *a* molecule, as shown in Fig. 1. The pigment clusters are located in the hydrophobic cavity formed by the protein. The peptide primary sequences of the NH<sub>2</sub> and COOH terminal regions are largely (56%) homologous and form structurally almost identical domains, each consisting of eight alpha-helices. The holoprotein, including two lipid molecules, has a molecular weight of 38.1 kDa. Distances between peridinin within a single domain range from 4 to 11 Å, and the conjugated regions of the peridinin are in van der Waals contact (3.3–3.8 Å) with the tetrapyrrole rings of the Chl *a* molecules. The distance between the Mg atoms of the two Chl *a* molecules in each subunit is 17.4 Å. The absorption spectrum of PCP complex exhibits only one unresolved Q<sub>y</sub> band for the two Chl *a* molecules, indicating similar spectral properties. The PCP, whose X-ray structure has been determined is the main form from *A. carterae*, and is denoted as MFPCP. Along with the MFPCP, a minor component has also been reported which is eluted from an anion exchange column at high-salt concentration [2]. This form, denoted high-salt PCP (HSPCP), presents 31% identity in amino acid sequence with MFPCP and contains only six peridinin and two Chl *a* molecules. The X-ray structure of HSPCP has been determined (T. Schulte, F.P. Sharples, R.G. Hiller, E. Hofmann, Coordinates have been deposited in the Brookhaven Protein Data Bank under ID 2C9E, unpublished) [3]. It shows a large similarity with the MFPCP structure in terms of pigment arrangement, except for the absence of two symmetry related peridinin called PID612/PID622, according to the nomenclature of Hofmann et al. of MFPCP (Per612–Per622 in Fig. 1). These two peridinin have been assigned to have blue-shifted absorption in the MFPCP complex [4]. Moreover, an interesting difference between MFPCP and HSPCP complexes is a splitting of the Chl *a* Q<sub>y</sub> band at low temperature in the HSPCP complex showing the local effect of the protein in determining the Chl *a* absorption properties. In MFPCP the two domains are not identical giving potentially eight peridinin environments [4].

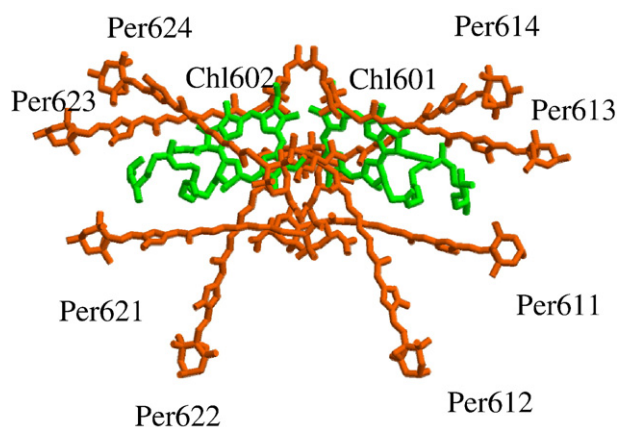


Fig. 1. Structure of the pigments associated with the monomeric basic unit of the PCP complex from *A. carterae*. Structure taken from coordinates of PCP complex 1 PPR deposited in the Brookhaven Protein Data Bank by Hofmann et al. [1] Pers correspond to PID in the PDB files, the numbering is maintained.

After the publication of the X-ray structure the number of spectroscopic studies on PCP proteins, aimed to correlate the spectroscopic properties to the arrangement of the pigments in the protein, increased quickly. The analysis of the absorption spectrum of the MFPCP together with those of circular dichroism (CD), linear dichroism (LD), and triplet-minus-singlet (T-S) spectra at low temperature, provided evidence for spectrally distinct peridinin with different 0–0 origins at 520, 537, and 555 nm [5]. Except for one missing spectral band, this result was in agreement with the results previously obtained by Carbonera et al. based on the simulation of the low temperature CD and absorption spectra, which were done taking into account the excitonic interactions among all pigments in PCP, and assuming 0–0 origins of peridinin at 485, 518, 534, and 543 nm [6]. Similar results were also obtained by fitting the 10 K absorption spectrum of MFPCP using absorption spectra of individual pigments taken at 10 K in 2-MTHF and shifted one to respect the other [7], [4]. The best fit was achieved in this way with three different peridinin located at 523, 528, and 545 nm (0–0 origins), in both subclusters, and with a fourth peridinin exhibiting different absorption in the two domains, peaking at 485 and 465 nm, respectively. These last two distinct blue-shifted spectra were assigned to peridinin 612 and 622 in the structure.

The S<sub>2</sub> states of peridinin are believed to couple excitonically, as suggested initially by CD spectra [8] and later by calculations based on the structure [6]. More recently Damjanovic et al. proposed a scheme of singlet excitation transfer and energy funneling in PCP: through light-absorption peridinin are excited into their S<sub>2</sub> states, which are excitonically coupled among all four peridinin. Per611, Per613, and Per614 retain the energy and convert it to their respective S<sub>1</sub> excitations. Excitation of the S<sub>1</sub> state of Per612 is prevented, since the occupancy of its S<sub>2</sub> state is low. The S<sub>1</sub> states are not excitonically coupled, but transfer individually to the Q<sub>y</sub> state of Chl601 [9].

Carotenoids bound to the light harvesting complexes of bacteria, plants and algae and having more than seven double bonds in the conjugated polyene chain, possess low-lying triplet states capable of trapping (B)Chl *a* triplet states avoiding the formation of the potentially harmful singlet oxygen and quenching active oxygen species [10]. Also peridinin molecules in the PCP complex are able to play this photo-protective role, with 100% efficiency in terms of triplet–triplet energy transfer. The dynamics of the peridinin triplet state in the PCP complex was determined to be 17±7 ns for the rise and 10±1 μs for the decay [11]. Triplet energy transfer has a very stringent distance requirement because it involves vanishingly small transition dipole moments associated with the spin-forbidden S<sub>0</sub>→T<sub>1</sub> transitions. Close proximity, essentially van der Waals contact between pigments, is required for efficient transfer. Inspection of the relative geometry of the Chl–peridinin couples in the structure lead Bautista et al. to state that the distance requirement is satisfied by per 1 and per 1' (corresponding to Per614, Per624 in Fig. 1) more than any of the other peridinin, making these the most likely energy traps for the Chl triplet (<sup>T</sup>Chl) states that are formed [11]. The analysis of the Triplet-minus-Singlet spectrum of PCP done by Kleima et al. [5] lead the authors to the conclusion that the observed T-S maxima

most likely corresponded to individual peridinin all contributing to the triplet quenching of the  $^1\text{Chl}$ . By combining T-S, OD, LD, and CD data the authors found evidence for four spectrally distinct peridinin having their electronic transitions at 520, 529 or 537, 546, and 555 nm. The source of the different spectroscopic properties, was assigned to site energy since each of these peridinin experiences a slightly different local environment in the protein. However an attempt to simulate the T-S spectrum in term of localization of the triplet state in one (o more) peridinin starting from a singlet excitonic state, was not considered.

Previous work based on Optically Detected Magnetic Resonance (ODMR) suggested that triplet–triplet energy transfer among peridinin molecules may take place in PCP complexes. The system was discussed as a multistate Frenkel exciton system performing stochastic jumps from one exciton state to another [12].

In conclusion, as for the singlet electronic states, there is not a clear picture of the triplet states of the peridinin in the PCP complex and the following main questions are still open: is there a specific peridinin in PCP devoted to the photo-protective mechanism? Is the triplet state localized in one specific peridinin in the complex? Is the triplet–triplet energy transfer among peridinin possible and, in the upper limit, must excitons states be considered?

To answer these questions we present here a new approach, based on time-resolved EPR (TR-EPR), to get insights into the nature of the peridinin(s) triplet state(s) in PCP. The approach exploits the concept of spin conservation during triplet–triplet energy transfer [13,14] which leads to spin polarization conservation. Actually the triplet–triplet mechanism is based on the exchange interaction, an operator which has not effect on the spin angular momentum. This means that the acceptor triplet state is formed in its three spin sublevels with probabilities which are given by the squares of the projections of the donor spin directions on the principal magnetic axes of the acceptor. In other words the polarization of the TR-EPR spectrum of the acceptor inherits the polarization of the donor in a way which depends on the relative geometrical arrangement of the donor–acceptor couple. Starting from the initially populated  $^1\text{Chl}$  and taking the relative positions among Chls and peridinin as in the X-ray structure we calculated the expected triplet state TR-EPR polarization of any peridinin in the complex. Comparison with the experimental data allows us to suggest a path for triplet quenching in PCP and answer the above raised questions.

## 2. Materials and methods

### 2.1. Sample preparation

*MFPCP* and *HSPCP* proteins, extracted and purified according to Sharples et al. [2], were kindly supplied by R.G. Hiller. Oxygen was removed from the samples by flushing argon in the EPR capillary before freezing. Glycerol, previously degassed by several cycles of freezing and pumping, was added (60% v/v) to obtain a transparent matrix.

### 2.2. TR-EPR measurements

TR-EPR spectra were obtained in direct detection mode using pulsed light excitation. The X-band EPR spectrometer (Bruker ECS106) was equipped with a TE<sub>102</sub> cavity (9.4 GHz) and a nitrogen flow system. For measurements at

cryogenic temperatures an Oxford helium cryostat (ESR 200) was used. Laser excitation at 532 nm (10 mJ per pulse and repetition rate of 10 Hz) was provided by the second harmonic of a Nd:YAG laser (Quantel Brilliant). To avoid magneto-phoselection due to the polarized laser beam, a lens to defocus the ray and hot filters covered with a clear mylar sheet were used before the sample to depolarize the light. The time resolution of the TR-EPR spectrometer was  $\sim 200$  ns. The microwave power used for the TR-EPR experiments was about 20 mW at the cavity. No field modulation or phase-sensitive detection was used. The EPR signals were taken from the microwave preamplifier (ER047-PH Bruker, bandwidth 20 Hz–6.5 MHz) and sampled with a LeCroy LT364 oscilloscope (1 ns per point). To eliminate the laser background signal, transients were accumulated under off-resonance field conditions and subtracted from those on resonance. The spectra at different times after the laser pulse were reconstructed from kinetic traces for each field position.

Triplet–triplet energy transfer has been calculated by a home-written program in Mathematica® software following the formalism of ref. [14] for the estimation of the acceptor populating rates starting from those of the acceptor in the limit of a triplet–triplet energy transfer which is fast, compared to the time evolution of the donor triplet spectrum and it is slow enough to allow spin alignment in the external magnetic field. Referring to the three triplet sublevels in zero magnetic field, the relationship between the populations of the acceptor and those of the donor is the following:

$$P_i^A = \sum_j \cos^2 \vartheta_{ij} P_j^D \quad (1)$$

where  $\vartheta_{ij}$  is the angle between the principal axis  $j$  of the donor and the axis  $i$  of the acceptor. In the presence of an external magnetic field the populating rates of the three sublevels at any field positions, which determine the initial polarization of the acceptor triplet state, can be calculated starting from those of the Zero field [14].

Although the absolute values of the donor populating rates are usually not known, and only relative  $P_x:P_y:P_z$  values are accessible by the experiments, it can be demonstrated that the relative population rates of the acceptor, which actually determine the shape of the TR-EPR spectrum, can be calculated directly

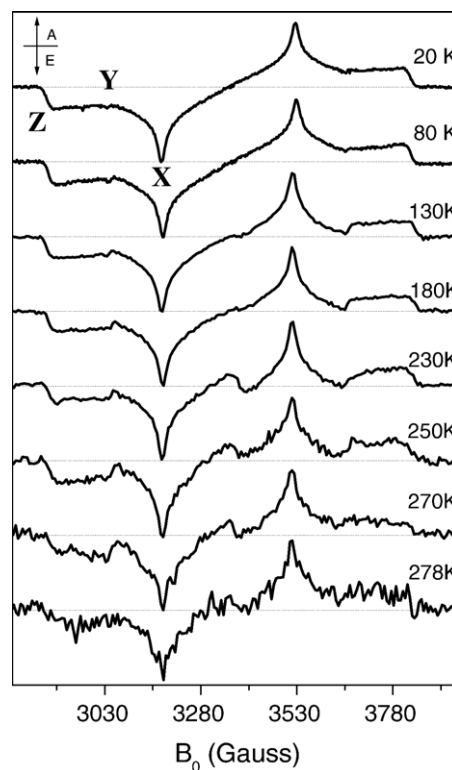


Fig. 2. TR-EPR spectra of PCP taken 250 ns after the laser pulse at different temperatures, as indicated. Order of energy for zero field triplet sublevels:  $|Z\rangle > |Y\rangle > |X\rangle$ .



from the above reported equation, using the relative  $P_j^D$  values. The absolute intensity of the acceptor spectrum cannot be estimated.

Simulations of the powder spin polarised triplet spectra were performed using a program written in MatLab® with the aid of the Easyspin routine (ver. 2.6.0) [15]. The program is based on the full diagonalization of the spin Hamiltonian, taking into account the Zeeman and magnetic dipole–dipole interactions, assuming a powder distribution of molecular orientations with respect to the magnet field direction.

### 3. Results

Fig. 2 shows the X-band spin-polarized EPR spectra of PCP at 250 ns after the laser pulse in the temperature range 20–273 K. The TR-EPR spectrum, simulated with the following values of the ZFS parameters:  $|D|=472$  G and  $|E|=42$  G, can be easily assigned to the carotenoid(s) present in the protein, the peridinin(s), on the basis of the comparison with the values of the ZFS parameters reported in previous ODMR work performed on the same protein [12]. The polarization pattern, *eeaeae*, remained unchanged up to physiological temperatures. The absence of  $^1\text{Chl}$  in the TR-EPR spectrum is in agreement with the value of 100% efficiency of triplet-quenching in PCP previously reported [11]. The triplet–triplet energy transfer from Chl to peridinins occurs in PCP in about 17 ns [11]. The time resolution of our set-up is about 200 ns. This means that we are able to detect only the acceptor triplet state, that is the carotenoid. On the other hand, the time evolution of the EPR-signal of the acceptor is slow compared to its formation, 3 to 40 micros depending on the zero field principal axis direction, so that we may consider the first detected spectrum at 250 ns as the “initial” spectrum which maintains the polarization inherited from the donor  $^1\text{Chl}$ .

As we have already stated we want to analyse the peridinin acceptor triplet state in terms of a triplet–triplet energy transfer from the  $^1\text{Chl } a$  donor. The fast time of the transfer (17 ns) allows to state that the initial polarization pattern of  $^1\text{Chl } a$  does not evolve significantly under the effect of spin relaxations before the transfer to the peridinin(s). Since we are not able to directly detect the  $^1\text{Chl}$ , being the transfer too fast for the time resolution of the set-up, we have to make some assumptions in terms of the sub-level populations of the  $^1\text{Chl } a$ .

In the literature there are mainly two different sets of Chl triplet populations which have been reported from in vitro studies, depending on the polarity of the solvent and on the ligation state of the central Mg [16–18]. The  $^1\text{Chl } a$  spectra, calculated with these two sets of populating rates, reported in Table 1, are shown in Fig. 3. They differ to each other in the polarization (*eeaeae* vs. *eeaeae*). In order to obtain some experimental evidence for the initial  $^1\text{Chl } a$  polarization pattern in the complex, we treated our samples with increasing amounts of the non-ionic detergent TritonX-100, up to 5 mM. This was done in order to “disturb” the triplet–triplet energy transfer between Chl and peridinin and decrease the efficiency of the transfer itself without perturbing too much the folding of the protein and the assembly of the pigments. By adding 2 mM detergent to the sample, we obtained a TR-EPR spectrum in which both the peridinin and the chlorophyll triplet states are visible. The spectrum is shown in Fig. 4. The comparison between the CD spectra of untreated and of the detergent-

Table 1  
Parameters of peridinin triplet state simulations

	Subcluster 1				Subcluster 2			
	Per 611	Per 612	Per 613	Per 614	Per 621	Per 622	Per 623	Per 624
$^1\text{Chl } a: P_x:P_y:P_z=0.37:0.41:0.22$								
$P_x$	0.33	0.25	0.36	0.22	0.27	0.25	0.37	0.23
$P_y$	0.28	0.38	0.26	0.38	0.33	0.39	0.24	0.38
$P_z$	0.39	0.37	0.38	0.40	0.40	0.36	0.39	0.39

$^1\text{Chl } a: P_x:P_y:P_z=0.33:0.56:0.11$

$P_x$	0.28	0.17	0.33	0.13	0.21	0.19	0.33	0.13
$P_y$	0.21	0.44	0.18	0.40	0.26	0.45	0.16	0.41
$P_z$	0.51	0.39	0.49	0.47	0.53	0.36	0.51	0.46

$|D|=479\pm0.5$  G

$|E|=46\pm0.5$  G

$W_x=20\pm1$  G

$W_y=10\pm1$  G

$W_z=10\pm1$  G

$\nu=9.413$  GHz;

$g_{\text{iso}}=2.0023$

This table reports the values of the population  $P_x, P_y, P_z$  of the triplet state of each peridinin present in PCP, calculated on the base of the spin conservation during triplet–triplet energy transfer, starting from two sets of  $^1\text{Chl } a$  sublevel populations as indicated. The others parameters used for the spectra simulation of peridinin triplet states are also reported: the ZFS parameters  $|D|$  and  $|E|$ , the linewidths  $W$ , at the canonical positions in the EPR powder spectrum, the frequency  $\nu$  of the spectrometer, and the isotropic  $g$  value.

treated samples is shown in the inset of Fig. 4, in the 300–700 nm range were only the pigments give contribution. The detergent-treated sample shows a decreased intensity of the CD spectrum, however the main features of the interactions among pigments are still present, although the relative intensity of the peaks is not maintained. Moreover the protein folding is conserved, as proven by the comparison of the CD spectra of the samples in the 190–300 nm spectral region, where the alpha-helix contribution prevails (not shown). The best reconstruction of the TR-EPR spectrum of the detergent-treated sample has been obtained with two triplet contributions: a peridinin triplet having the same polarization than the untreated sample and a  $^1\text{Chl}$  with an *eeaeae* polarization pattern. In summary the  $^1\text{Chl } a$  appearing in the detergent treated samples is similar to that reported in Fig. 3 (dotted line,  $P_x:P_y:P_z=0.37:0.41:0.22$ ). Although, on the basis of the experiments with the detergent, we favour the choice of this Chl  $a$  triplet polarization, we make calculations of the acceptor populating rates using both the spectral patterns reported in Fig. 3. In fact, as we will see in the outcome of the calculations, the choice is not important for the main conclusions that can be drawn from the results.

The other parameters necessary in performing the calculations of the triplet–triplet energy transfer are the directions of the ZFS axes, with respect to the molecular frames of the two partners (see equation in Materials and methods). The  $^1\text{Chl } a$  ZFS axes have been chosen as shown in Fig. 5, according to literature data [19,20]. The ZFS axes of the peridinin triplet state have been chosen analogously to those determined for beta-carotene in crystals [21,22]. The long axis is the Z axis while the X axis is along the C–H bonds in the conjugated chain. The Y

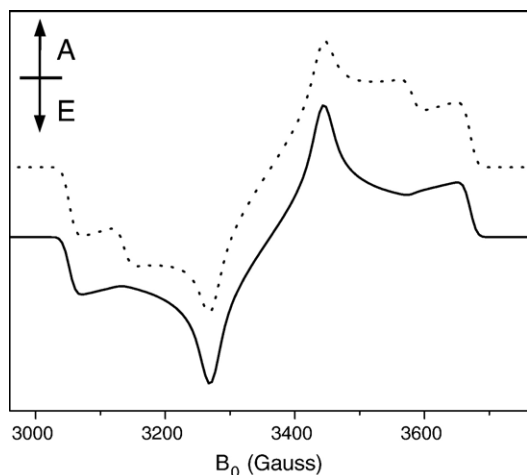


Fig. 3. Simulated TR-EPR spectrum of  $^3\text{Chl } a$  with populating rates corresponding to:  $P_x:P_y:P_z=0.37:0.41:0.22$  (upper dotted trace) and  $P_x:P_y:P_z=0.33:0.56:0.11$  (bottom line). Order of energy for zero field triplet sublevels:  $|Z\rangle>|X\rangle>|Y\rangle$ .

direction is perpendicular to the conjugated XZ molecular plane. Since the peridinin are slightly distorted in the X-ray structure we calculated the mean plane with respect to the all carbon atoms belonging to the conjugated system and chose the long axis laying in such a plane and passing through the carbon atoms of the polyene chain contained in the  $\pi$ -plane (see Fig. 5). All the relevant geometrical parameters are reported in the Supplementary material.

With these assumptions and parameters we calculated the peridinin spectra for all the eight Chl  $a$ -peridinin mutual configurations reported in the X-ray structure. In spite of the pseudo  $C_2$  symmetry-relating the two subclusters of pigments in the protein complex, the relative position of the homologous Chl-peridinin couples is not identical and little difference in

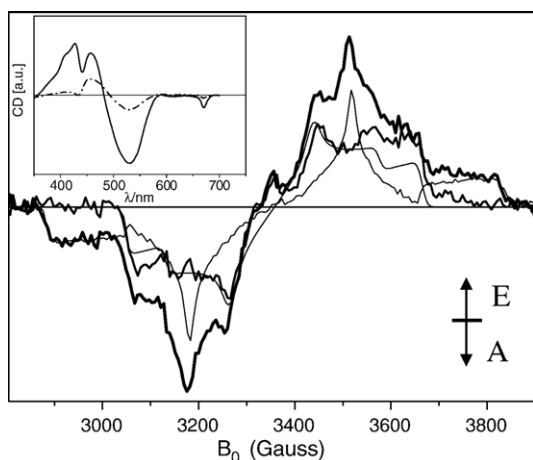


Fig. 4. TR-EPR spectra of PCP taken 250 ns after the laser pulse, at 130 K. 2 mM Triton X100 was added to the sample. The spectrum obtained as difference of the detergent-treated minus a certain percentage (about 50%) of the untreated spectrum is shown as inner thick line, and is compared to the chlorophyll triplet spectrum simulated with the values  $P_x:P_y:P_z=0.37:0.41:0.22$  already reported in Fig. 3. The spectra of untreated PCP sample and of Chl  $a$  are shown as thin lines. Inset: CD spectra of untreated (solid line) and detergent-treated (dashed-dot) PCP.

mutual configurations must be considered in the calculations. As an example, the difference between the geometry of one symmetry related couple is shown in Fig. 5.

Excitation dynamics with time constants of  $6.8\pm0.8$  ps and  $350\pm15$  ps were assigned to equilibration times among Chls within the monomer and within the trimer, respectively [23]. More recently, the difference in energy between the two  $Q_y$  absorption bands of the two Chls of the monomer has been estimated to be about 5 nm (670 vs. 675 nm) [24]. Given the little energy difference and the invariability of the TR-EPR spectrum with the increase in temperature, both Chls in each PCP monomer are likely to be involved in triplet formation and triplet quenching with comparable probability. However, for the sake of completeness, we considered all the three possibilities: (a) the  $^3\text{Chl}$  is formed only in the subcluster 1; (b) the  $^3\text{Chl}$  is formed only in the subcluster 2; (c)  $^3\text{Chls}$  are formed in both the subclusters.

In Fig. 6, we report the calculated spectra, in which the contributions of the two symmetry related pairs in the PCP monomer were summed with the same percentage, and compared to the experimental spectrum. The results for each single subcluster are shown in the Supplementary material. No significant differences between the two subclusters were found, meaning that, on the basis of TR-EPR data, we are not able to distinguish if the triplet transfer occurs preferentially in one of the two subcluster or in both with different or equal probability.

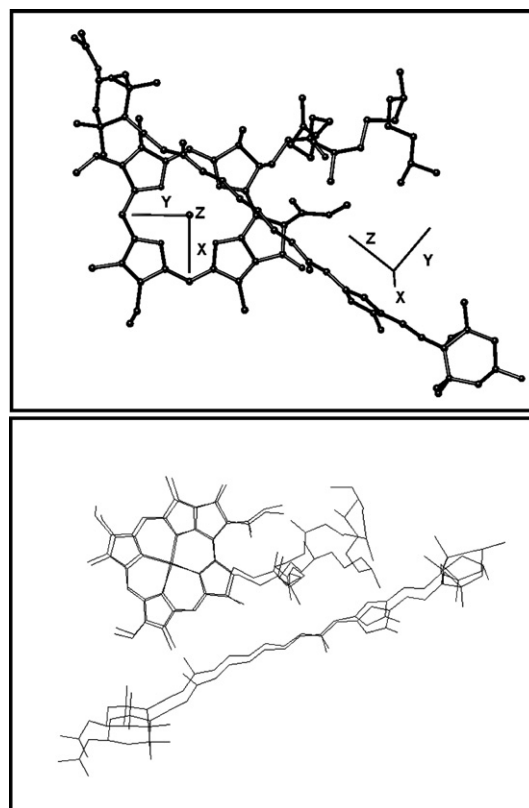


Fig. 5. ZFS axes directions of Chl  $a$  and peridinin triplet states with respect to the molecular structure are shown in the upper panel. As an example the couple Chl601–Per614 is represented. Bottom panel: overlap of two Chl–Per pairs related by the  $C_2$  symmetry in PCP complex. The Chl601–Per611 and the Chl602–Per621 pairs are shown as example of differences in relative geometry.

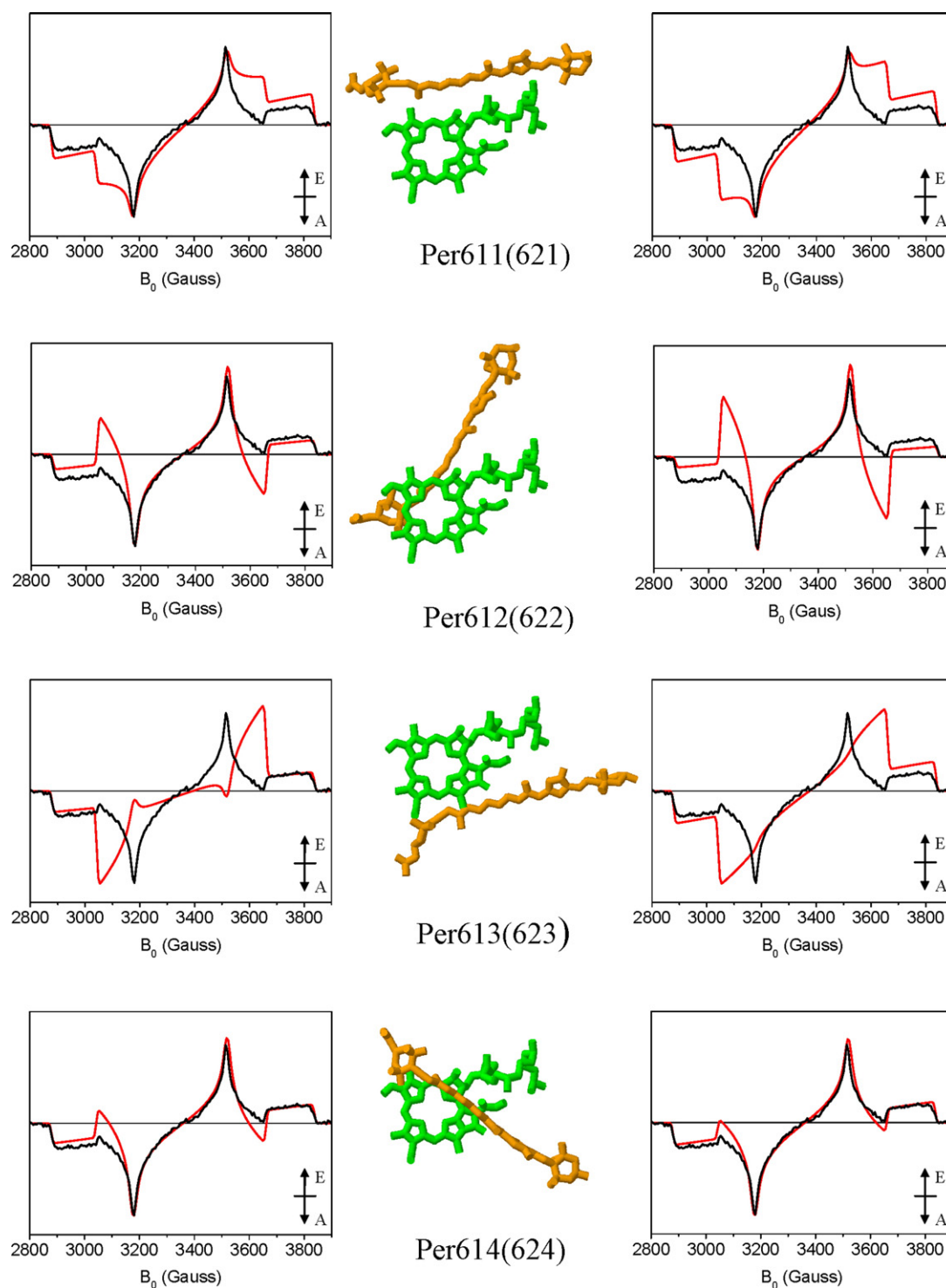


Fig. 6. Calculated TR-EPR spectra of peridinins for two sets of initial relative populations of  $^T\text{Chl}$ : left,  $P_x:P_y:P_z=0.37:0.41:0.22$ ; right  $P_x:P_y:P_z=0.33:0.56:0.11$ . Other parameters are reported in Table 1. The spectra represent the sum of the contributions of the two subclusters for each Chl–Per couple. Each calculated spectrum is compared to the experimental one taken at 130 K and already reported in Fig. 2. In the figure the structure of each pair in one subcluster is also shown to point out the differences in the geometrical arrangements.

Inspection of the results reported in Fig. 6 allows to state that the calculated spectrum has the same polarization pattern (*eaeaea*) as the experimental one only for two mutual arrangements of the Chl–peridinin pigments, independently from the initial populations pattern chosen for the  $^T\text{Chl } a$  in the calcu-

lations. These arrangements correspond to the pairs Per612 (622)–Chl601(602) and Per614(624)–Chl601(602), the latter giving a better agreement with the experiments.

The TR-EPR spectrum of the HSPCP is shown in Fig. 7. It is identical to the spectrum of the MFPCP. Given that the reported

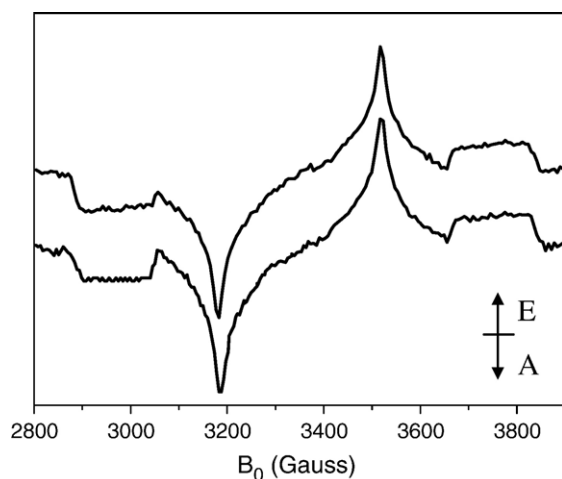


Fig. 7. TR-EPR spectra of MFPCP (upper trace), and HSPCP (bottom trace) taken 250 ns after the laser pulse.  $T=130$  K.

X-ray structure of the HSPCP shows a large similarity with the MFPCP structure in terms of pigment arrangement, except for the absence of two symmetry related peridinin (Per612 and Per622), we can reasonably assume that Per612(622) cannot give the main contribution to the TR-EPR spectrum even in the

MFPCP. On the basis of this analysis, Per614(624) remains the best candidate for the efficient triplet quenching observed in PCP, when considering localization of the triplet state in a single peridinin in each subcluster.

However we must also consider the possibility that the experimental triplet spectrum is derived from the contributions of more peridinin in the complex. This would be suggested by the analysis done by [5] of the T-S spectrum in terms of different triplet states assigned to the peridinin in the complex. By summing the spectra calculated for the eight different peridinin triplet states, following the hypothesis that they are populated directly from the nearby  $^1\text{Chl}$ , and excluding Per612(622) because of the results obtained with the HSPCP, we found that, to fit the experimental TR-EPR spectrum of PCP, the contribution of Per614(624) must be at least 80%–60% in whatever sum considered. Per613(623) and Per611(621) may be considered alternatively with a contribution of about 20–40% respectively, or together with a relative contribution of 20% each. The results obtained by summing the contributions of both subclusters are shown in Fig. 8. The results relative to single subclusters are reported in the Supplementary material.

Another possibility which must be taken into account is that the triplet, initially populated by direct transfer from the  $^1\text{Chl}$  in a specific peridinin, further migrates to a different one. The

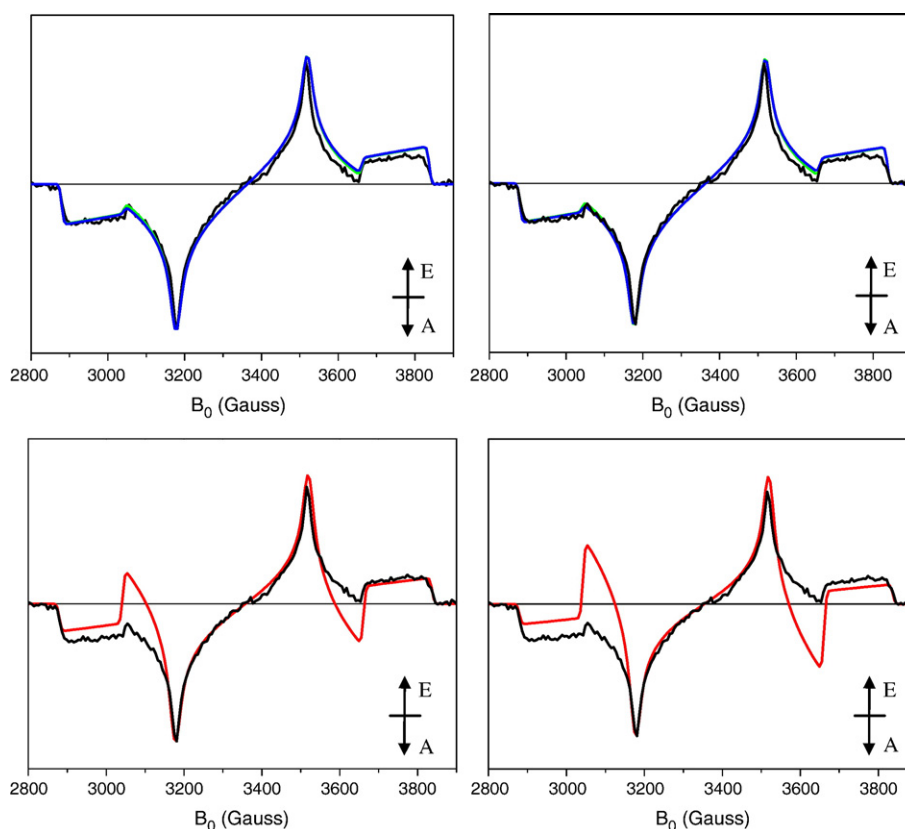


Fig. 8. Calculated TR-EPR spectra of peridinin for two sets of initial relative populations of  $^1\text{Chl}$ ; left:  $P_x:P_y:P_z=0.37:0.41:0.22$ ; right:  $P_x:P_y:P_z=0.33:0.56:0.11$ . Other parameters as in Table 1. Each calculated trace represents the sum of the contributions of the two subclusters for each Chl–Per couple. Upper panels: left: spectra calculated by summing either  $^1\text{Per614(624)}+0.75\cdot^1\text{Per611(621)}$  (green) or  $^1\text{Per614(624)}+0.3\cdot^1\text{Per613(623)}$  (blue); right: spectra calculated by summing either  $^1\text{Per614(624)}+0.30\cdot^1\text{Per611(621)}$  (green) or  $^1\text{Per614(624)}+0.25\cdot^1\text{Per613(623)}$  (blue). The calculated spectra, which are almost coincident, are compared to the experimental ones in the same panel. Bottom panels: spectra calculated (red) for the multiple triplet–triplet energy transfer  $^1\text{Chl601(602)}\rightarrow^1\text{Per613(623)}\rightarrow^1\text{Per614(624)}$  in comparison with the experimental one. (For interpretation of the references to colour in this figure legend, the reader is referred to the web version of this article.)



transfer, if there is one, should take place in a fast time scale compared to TR-EPR time resolution because there is not evidence for this process in the time evolution of the spectrum (not shown). By considering all the different couples of peridinin for the triplet migration, we found that only the transfer Per613(623)→Per614(624) gives rise to a spectrum with the same polarization pattern *eaeaea* as the experimental one. However, agreement with the experiments is poor, as can be seen in Fig. 8. Multiple jumps do not improve the fitting (not shown).

#### 4. Discussion

In PCP the photo-protective role is played by peridinin with 100% efficiency. Triplet energy transfer has a very stringent distance requirement and is very sensitive to the mutual orientation of the molecular  $\pi$  orbitals of the molecules involved. Therefore, little differences in the relative geometry of the donor–acceptor pair may lead to a preferential pathway in the triplet quenching. In the PCP complex the presence of several peridinin surrounding the Chl *a* molecules, at comparable shortest distances of the conjugated molecular systems, makes the question about the most favourable way of triplet quenching not trivial. Spin conservation during triplet–triplet energy transfer can be exploited for gaining insights into the structural requirements for efficient triplet–triplet energy transfer in the structure of the complex. Spin conservation is not observed in systems in which the triplet–triplet energy transfer occurs is a time scale which is too short to allow the spin alignment with respect to the external magnetic field [14]. In X-band EPR this limit is about 20 ps. Since the peridinin triplet rise time is 17 ns [11], the condition of spin conservation is fulfilled.

The analysis reported in the Results section shows that the initial polarization of the triplet state detected in PCP may be reproduced well by considering a single Triplet transfer step from Chl601 to Per614 in one subcluster and from Chl602 to Per624 in the other. It is worth noting that this result does not depend critically on the assumptions that have to be made to perform the calculations. A possible source of inaccuracy in the calculations could be the choice of the directions of the ZFS axes of the peridinin molecules due to the fact that the peridinin are slightly distorted in the X-ray structure and that the triplet state geometry could be different with respect to that of the ground state. To test the sensitivity of the analysis to this initial choice, we also calculated the spectra for ZFS axes rotated  $\pm 30^\circ$  about the *X*, *Y*, *Z* axes shown in Fig. 5. Within  $\pm 20^\circ$  the polarization pattern of the calculated spectrum did not change significantly. To obtain agreement with the TR-EPR experiments there is no need to involve more than Per614(624) in the quenching. The results, however, are also consistent with a contribution of others peridinin to the observed spectrum, namely Per611(621) (up to 40%) and, at less extent, Per613(623) (up to 30%). Still, Per614(624) remains the main site of triplet quenching. The role of Per612(622) in the triplet quenching is ruled out by the fact that its absence, as in the HSPCP complex, did not alter the features of the spectrum. This is also consistent with the fact that Per612/Per622 have a blue-shifted absorption spectrum in the MFPCP

complex because of their unfavourable site energy [4]. Therefore their triplet state are also likely to be located at higher energy with respect to the other peridinin, making them less efficient for the trapping of the  $^1\text{Chl } a$ .

In the temperature range investigated by TR-EPR experiments, up to 273 K, the spectrum does not change significantly. This means that the triplet–triplet energy transfer between Chl and peridinin is not temperature-dependent and is in agreement with the 100% efficiency of triplet quenching observed already at cryogenic temperatures [12,25,26]. Furthermore, the absence of temperature effects on the initial polarization of the TR-EPR spectrum of PCP makes the possibility of triplet–triplet energy transfer among peridinin in the time scale of 100–200 ns unlikely, while in the time scale of micros, which is accessible to our experiments, there was no evidence of triplet transfer. This was also confirmed by the calculations of the spectra based on the hypothesis of triplet–triplet energy transfer among close peridinin. In fact the calculated spectra showed poor agreement with the experimental ones.

Finally we want to discuss the possibility of having coherent triplet exciton in the peridinin cluster(s). The analysis of our previous work based on Optically Detected Magnetic Resonance (ODMR) experiments performed on PCP, showed that triplet exchange among peridinin could be already active at very low temperature (1.8 K) [12]. The experimental evidence of triplet exchange was the merging of two ODMR transitions into one and a frequency shift of the resonance lines by increasing the temperature [26]. However very small energy differences between the excitonic triplet states (10 to 40  $\text{cm}^{-1}$ ) and large electronic couplings (0.8  $\text{cm}^{-1}$  intra-subcluster and 0.35  $\text{cm}^{-1}$  inter-subcluster) were needed to account for the experimental effects in a coherent triplet exciton description of the system. These values now seem to be inadequate in view of the estimated site energies of the singlet states made by Kleima et al. [5] which makes the localization of the triplet state a probable event to occur in PCP. Moreover we have recently performed several ODMR studies on other antenna complexes where carotenoids are populated by quenching of Chl triplet states [27], and on synthetic carotene-porphyrin molecular dyads (unpublished data), and found that ODMR frequency shifts, narrowing and merging of lines of the carotenoid triplet states, were present. In such systems no exciton interaction among carotenoids was expected because of the large distance among pigments. Therefore, we suggest that the internal dynamics of the carotenoid molecule, rather than exchange between different carotenoids, should be considered in order to

Table 2  
Relevant chlorophyll–peridinin distances in PCP

	$\pi$ – $\pi$ shortest distance (Å)	Center to center distance (Å)
Chl–Per611/621	4.38/4.50	8.57/8.57
Chl–Per612/622	4.24/3.70	8.97/8.97
Chl–Per613/623	4.24/4.14	9.36/9.49
Chl–Per614/624	5.00/4.71	5.44/5.36

The table reports the significant distances between the peridinin and the chlorophyll molecules obtained from coordinates of PCP complex, 1 PPR deposited in the Brookhaven Protein Data Bank by Hofmann et al. [1].



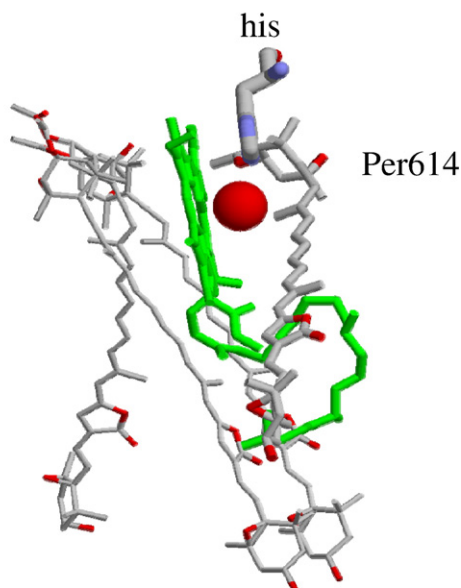


Fig. 9. Structure of the pigments associated with one subcluster of the PCP complex from *A. carterae*. Per614, Chl601 and the Mg-coordinated water molecule, together with the his close to it, are shown in a thick wireframe. Structure taken from coordinates of PCP complex 1 PPR deposited in the Brookhaven Protein Data Bank by Hofmann et al. [1].

account for the ODMR spectral changes observed by increasing the temperature. We carefully analysed the line-shape, the ZFS positions, and the time evolution of the TR-EPR spectra taken in the temperature range 20–273 K searching for evidence of the exciton dynamics but found no elements supporting such a mechanism. The analysis of the TR-EPR spectrum reported in the Results section of this work strongly suggests that the triplet state populated from the Chl *a* molecules is localized mainly in the Per 614(624) site(s). On the basis of this, we think that also the T-S spectrum should be re-discussed in terms of localization of the triplet state and change of the electronic coupling among the peridinin in their singlet states upon triplet formation. This approach, which has not been adopted yet in describing the T-S spectrum of PCP even in the most recent papers [5,9], has been used, for instance, to successfully discuss the T-S spectrum of the FMO protein. FMO is an antenna complex of green sulfur bacteria in which seven BChls interact to give rise to excitonic states in the singlet but not in the triplet manifold, the triplet state being localized in a specific BChl *a* [28].

It is interesting to look for a correlation between the specific pairs Chl601(602)–Per614(624) identified by our results as the active ones in the photo-protective mechanism and the structural requirements for efficient triplet–triplet energy transfer as indicated by the X-ray structure. The triplet–triplet energy transfer process is based on the Dexter mechanism. The efficiency of the process depends on the overlap between the wavefunctions of the donor and the acceptor. All the peridinin are in Van der Waals contact with the Chl *a* molecular rings and have comparable  $\pi$ – $\pi$  shortest distances. What differentiates Per14(624) from the others is the closest center-to-center distance (see Table 2). Inspection of the relative geometry of the

Chl–peridinin couples in the structure lead Bautista et al. [11] to state that the distance requirement is satisfied by per 1 and per 1' (corresponding to Per614, Per624 in the nomenclature we have adopted) more than any of the other peridinin. In contrast Damjanovic et al. calculated the exchange couplings and transfer times and found that the most favoured is Per613 ( $5.93 \times 10^{-4}$  eV, 298 ps) followed by Per614 ( $3.7 \times 10^{-5}$  eV, 76.9 ns) [9]. Our results disagree with this latter prediction. It is worth noting that a unique feature which characterizes Per614(624)–Chl601(602) pair(s) is that the 5th ligand of the central Mg of the Chl is a water molecule which is placed in between this pair (see Fig. 9). The water molecule can play a role in the extension of the overlap between Chl and peridinin, and may act as a bridge in the transfer. It is known that the overlap between wavefunctions may become critical at even shorter distances for triplet–triplet transfer compared to Electron Transfer [29,30]. Therefore super-exchange models involving a bridge, or the medium, interposed between the donor and the acceptor molecules become important for describing also triplet–triplet energy transfer, especially for expected small vacuum couplings between the couple involved in the transfer [31,32].

In the case of PCP there is no evidence from the X-ray structure of either molecular or protein bridges connecting the peridinin to each other or to the Chls except for the water molecule mentioned above. This water molecule was not considered in the calculations by Damjanovic et al. but it could be the decisive factor in favouring the  $^1\text{Chl601(602)} \rightarrow ^1\text{Per614(624)}$  pathway. In this regard, it is interesting to note that Mao et al. found significant contribution of the water molecule to the intermolecular interaction energy of Per624–Chl602 using MP2/6-31G\* calculations [33].

In conclusion, the present work does not support the presence of triplet exciton on PCP and favours the hypothesis of localization of the triplet state mainly in one peridinin in each subcluster. In order to further investigate this issue and provide a map of the electronic distribution in the triplet state of peridinin, which will allow getting an estimation of the electronic coupling, we are presently performing ENDOR experiments on the triplet state of PCP. Preliminary results confirm the localization of the triplet state in the range 5–150 K (unpublished results).

## Acknowledgments

This work was supported by the Italian Ministry for University and Research (MURST) under the project PRIN2005. We are grateful to Prof. Giovanni Giacometti for his continuous interest in this work.

## Appendix A. Supplementary data

Supplementary data associated with this article can be found, in the online version, at doi:10.1016/j.bbabi.2007.09.002.

## References

- [1] E. Hofmann, P.M. Wrench, F.P. Sharples, R.G. Hiller, W. Welte, K. Diederichs, Structural basis of light harvesting by carotenoids: peridinin–chlorophyll–protein from *Amphidinium carterae*, *Science* 272 (1996) 1788–1791.

- [2] F.P. Sharples, P.M. Wrench, K.L. Ou, R.G. Hiller, Two distinct forms of the peridinin–chlorophyll  $\alpha$ –protein from *Amphidinium carterae*, Biochim. Biophys. Acta 1276 (1996) 117–123.
- [3] R.P. Ilagan, J.F. Kosciellecki, R.G. Hiller, F.P. Sharples, G.N. Gibson, R.R. Birge, H.A. Frank, Femtosecond time-resolved absorption spectroscopy of main-form and high-salt peridinin-chlorophyll proteins at low temperatures, Biochemistry 45 (2006) 14052–14063.
- [4] R.P. Ilagan, S. Shima, A. Melkozernov, S. Lin, R.E. Blankenship, F.P. Sharples, R.G. Hiller, R.R. Birge, H.A. Frank, Spectroscopic properties of the main-form and high-salt peridinin-chlorophyll  $\alpha$  proteins from *Amphidinium carterae*, Biochemistry 43 (2004) 1478–1487.
- [5] F.J. Kleima, M. Wendling, E. Hofmann, E.J.G. Peterman, R. van Grondelle, H. van Amerongen, Peridinin chlorophyll  $\alpha$  protein: relating structure and steady-state spectroscopy, Biochemistry 39 (2000) 5184–5195.
- [6] D. Carbonera, G. Giacometti, U. Segre, E. Hofmann, R.G. Hiller, Structure-based calculations of the optical spectra of the light-harvesting peridinin–chlorophyll–protein complexes from *Amphidinium carterae* and *Heterocapsa pygmaea*, J. Phys. Chem., B 103 (1999) 6349–6356.
- [7] E. Papagiannakis, M. Vengris, D.S. Larsen, I.H.M. van Stokkum, R.G. Hiller, R. van Grondelle, Use of ultrafast dispersed pump-dump-probe and pump-repump-probe spectroscopies to explore the light-induced dynamics of peridinin in solution, J. Phys. Chem., B 110 (2006) 512–521.
- [8] P.S. Song, P. Koka, B. Prezelin, F. Haxo, Molecular topology of the photosynthetic light-harvesting pigment complex, peridinin–chlorophyll  $\alpha$ –protein, from marine dinoflagellates, Biolog. Cybern. 15 (1976) 4422–4427.
- [9] A. Damjanovic, T. Ritz, K. Schulten, Excitation transfer in the peridinin–chlorophyll–protein of *Amphidinium carterae*, Biophys. J. 79 (2000) 1695–1705.
- [10] H.A. Frank, R.J. Cogdell, Carotenoids in photosynthesis, Photochem. Photobiol. 63 (1996) 257–264.
- [11] J.A. Bautista, R.G. Hiller, F.P. Sharples, D. Gosztola, M. Wasielewski, H. A. Frank, Singlet and triplet energy transfer in the peridinin–chlorophyll  $\alpha$ –protein from *Amphidinium carterae*, J. Phys. Chem., A 103 (1999) 2267–2273.
- [12] D. Carbonera, G. Giacometti, U. Segre, A. Angerhofer, U. Gross, Model for triplet–triplet energy transfer in natural clusters of peridinin molecules contained in Dinoflagellate's outer antenna proteins, J. Phys. Chem., B 103 (1999) 6357–6362.
- [13] M.A. El-Sayed, D.E. Tinti, E.M. Yee, Conservation of spin direction and production of spin alignment in triplet–triplet energy transfer, J. Chem. Phys. 51 (1969) 5721–5723.
- [14] K. Akiyama, S. Terokubota, T. Ikoma, Y. Ikegami, Spin polarization conservation during intramolecular triplet–triplet energy-transfer studied by time-resolved EPR spectroscopy, J. Am. Chem. Soc. 116 (1994) 5324–5327.
- [15] S. Stoll, A. Schweiger, EasySpin, a comprehensive software package for spectral simulation and analysis in EPR, J. Magn. Reson. 178 (2006) 42–55.
- [16] R.H. Clarke, Triplet State ODMR Spectroscopy. Techniques and Applications to Biophysical Systems, in: R.H. Clarke (Ed.), Wiley-Interscience, New York, 1982.
- [17] M.C. Thurnauer, ESR study of photoexcited triplet state in photosynthetic bacteria, Rev. Chem. Intermed. 3 (1979) 197–230.
- [18] R.H. Clarke, S. Hotchandani, S.P. Jagannathan, R.M. Leblanc, Ligand effects on the triplet state of chlorophyll, Chem. Phys. Lett. 89 (1982) 37–40.
- [19] J. Vrieze, A.J. Hoff, The orientation of the triplet axes with respect to the optical-transition moments in (bacterio)chlorophylls, Chem. Phys. Lett. 237 (1995) 493–501.
- [20] F. Lendzian, R. Bittl, A. Telfer, W. Lubitz, Hyperfine structure of the photoexcited triplet state P680 in plant PSII reaction centres as determined by pulse ENDOR spectroscopy, Biochim. Biophys. Acta 1605 (2003) 35–46.
- [21] J. Frick, J.U. Vonschutz, H.C. Wolf, G. Kothe, 1st detection of the (nonphosphorescent) triplet-state in single-crystals of beta-carotene, Mol. Cryst. Liq. Cryst. 183 (1990) 269–272.
- [22] J. Frick, PhD Thesis, Stuttgart, 1992.
- [23] F.J. Kleima, E. Hofmann, B. Gobets, I.H.M. van Stokkum, R. van Grondelle, K. Diederichs, H. van Amerongen, Forster excitation energy transfer in peridinin–chlorophyll- $\alpha$ -protein, Biophys. J. 78 (2000) 344–353.
- [24] M. Krikunova, H. Lokstein, D. Leupold, R.G. Hiller, B. Voigt, Pigment–pigment interactions in PCP of *Amphidinium carterae* investigated by nonlinear polarization spectroscopy in the frequency domain, Biophys. J. 90 (2006) 261–271.
- [25] D. Carbonera, G. Giacometti, U. Segre, Carotenoid interactions in peridinin chlorophyll  $\alpha$  proteins from dinoflagellates — evidence for optical excitons and triplet migration, J. Chem. Soc., Faraday Trans. 92 (1996) 989–993.
- [26] D. Carbonera, G. Giacometti, G. Agostini, FDMR spectroscopy of peridinin chlorophyll- $\alpha$  protein from *Amphidinium-carterae*, Spectrochimica 51A (1995) 115–123.
- [27] D. Carbonera, G. Agostini, T. Morosinotto, R. Bassi, Quenching of chlorophyll triplet states by carotenoids in reconstituted Lhca4 subunit of peripheral light-harvesting complex of photosystem I, Biochemistry 44 (2005) 8337–8346.
- [28] S.I.E. Vulto, M.A. de Baat, R.J.W. Louwe, H.P. Permentier, T. Neef, M. Miller, H. van Amerongen, T.J. Aartsma, Exciton simulations of optical spectra of the FMO complex from the green sulfur bacterium chlorobium tepidum at 6 K, J. Phys. Chem., B 102 (1998) 9577–9582.
- [29] G.L. Closs, M.D. Johnson, J.R. Miller, P. Piotrowiak, A connection between intramolecular long-range electron, hole and triplet energy transfer, J. Am. Chem. Soc. 11 (1989) 3751–3753.
- [30] G.L. Closs, P. Piotrowiak, J.M. MacInnis, G.R. Fleming, Determination of Long distance intramolecular triplet energy transfer rates. A quantitative comparison with electron transfer, J. Am. Chem. Soc. 110 (1988) 2652–2653.
- [31] J. Lin, I.A. Balabin, D.N. Beratan, The nature of aqueous tunneling pathways between electron-transfer proteins, Science 310 (2005) 1311–1313.
- [32] H.B. Gray, J.R. Winkler, Electron transfer in metalloproteins, in: V. Balzani, P. Piotrowiak, M.A.J. Rodgers, J. Mattay, D. Astruc, H.B. Gray, J. Winkler, S. Fukuzumi, T.E. Mallouk, Y. Haas (Eds.), Electron Transfer in Chemistry Wiley-VCH, vol.3, 2001, pp. 2–22.
- [33] L.S. Mao, Y.L. Wang, X.C. Hu, pi-pi stacking interactions in the peridinin–chlorophyll–protein of *Amphidinium carterae*, J. Phys. Chem., B 107 (2003) 3963–3971.